Phase Slips and Metastability in Granular Boron-doped Nanocrystalline Diamond Microbridges

G.M. Klemencic[a,*], D. T. S. Perkins[b], J. M. Fellows[c], C. M. Muirhead[b], R. A. Smith[b], S. Mandal[a], S. Manifold[a], M. Salman[a], S. R. Giblin[a], O. A. Williams[a]

[a] *School of Physics and Astronomy, Cardiff University, Queen's Buildings, The Parade, Cardiff, CF24 3AA, UK*
[b] *School of Physics and Astronomy, University of Birmingham, Birmingham, B15 2TT, UK*
[c] *School of Physics, HH Wills Physics Laboratory, University of Bristol, Tyndall Avenue, Bristol, BS8 1TL, UK*

BNCD film preparation

The boron-doped nanocrystalline diamond (BNCD) film was grown on a 2-inch SC-1 cleaned (100) silicon wafer with a 500 nm thick SiO_2 buffer layer using microwave plasma-assisted chemical vapour deposition in a Seki AX6500 series microwave plasma reactor system[1]. Before loading into the reactor chamber, the substrate was seeded for 10 min by ultrasonic agitation in a monodisperse aqueous colloid of nanodiamond particles[2], rinsed in deionised water, and spun dry. The film was grown in a gas mixture of 3% methane in hydrogen. The chamber pressure was 40 Torr, the microwave power was 3.5 kW, and the substrate temperature was 720 $^{\circ}$C during growth as measured by a dual wavelength pyrometer. The charge carriers required for superconductivity in diamond were provided by the addition of trimethylboron to the gas mixture with a B/C ratio of 12,800 ppm. If 100% incorporation efficiency from the gas phase is assumed, there is an upper limit of $2.3 \times 10^{21}\,\mathrm{cm}^{-3}$ for the carrier concentration. The film thickness was monitored during growth by *in situ* laser interferometry and subsequently measured by cross sectional scanning electron microscopy (SEM). The surface of the resulting 339 nm thick film is shown in Fig. 1. The film has a distribution of grain sizes, with a mean grain size of 102 nm and a surface

*Corresponding author
Email address: KlemencicG@cardiff.ac.uk (G.M. Klemencic)

roughness of ∼25 nm RMS. Previous work has shown that the surface roughness of the film does not affect the shape and magnitude of the superconducting transition[3].

Microbridge fabrication

The 1600 μm long microbridges of varying width (4.6, 6.7, and 10.5 μm) were fabricated from the 339 nm thick BNCD film using a standard top-down photolithographic approach. Microbridge structures were defined by thermal evaporation of a 70 nm nickel mask through patterned resist and subsequent lift-off in acetone. The exposed surrounding BNCD was etched by oxygen inductively coupled plasma reactive ion etching (ICP-RIE). The ICP power was 1500 W, the RIE power was 100 W, and the oxygen flow was 40 sccm. The metal mask was removed in $FeCl_3$ and thoroughly cleaned to remove all traces of the mask. The unpatterned sample is an approximately 5 mm square piece of the BNCD sample with the current and voltage leads arranged in a Van der Pauw configuration.

Measurement Techniques

Four-wire electrical contact to the microbridge samples was made by direct wire bonding to the surface and Ohmic contact behavior was confirmed. Resistance as a function of temperature, shown in Fig. 2, was measured using a Quantum Design Physical Property Measurement System. The excitation current was 0.5 μA, well below both $I_{c(min)}$ and $I_{c(max)}$ of all microbridges.

$V(I)$ characteristics were measured at 1.9 K in zero applied field using a bespoke battery-operated voltage-controlled current source and amplifier. The general behavior shown in Fig. 4 persists down to dilution refrigerator temperatures though with a corresponding increase in the achievable $I_{c(max)}$. Electromagnetic noise pulses were applied by either operating a small electrical motor close to the electrical measurement apparatus, or by summing the input bias signal with a pulse output by a second computer-controlled arbitrary waveform generator.

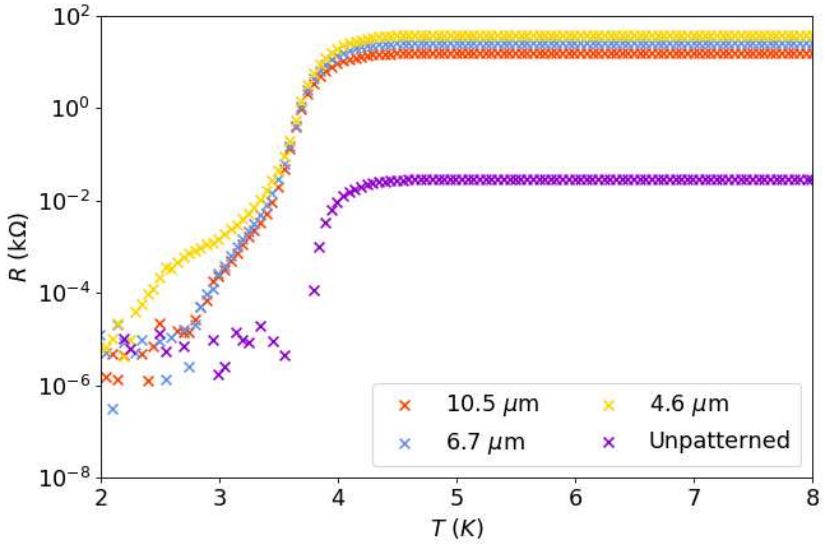

Figure 1: Resistance as a function of temperature, $R(T)$, for BNCD microbridges and the unpatterned film shown for the range 2–8 K.

Additional data

For completeness, the $R(T)$ and $V(I)$ graphs for the 4.6 and 10.5 μm microbridges are shown here. Fig. 1 (with detailed fits shown in Fig. 2 and 3) shows all three microbridge $R(T)$ curves together with that of the unpatterned film; an additional broadening is observed below T_c for the microbridge samples. This data does show a systematic dependence on bridge width, although it is impossible to make conclusive statements based on only three values of width. The phase slip shoulder in the $R(T)$ data becomes narrower as bridge width increases, as expected theoretically since the free energy barrier for a phase slip increases with width. Fig. 4 shows $V(I)$ data for these same microbridges, showing that similar discrete voltage steps are formed. Similarly, the current intercept I_0 in the $V(I)$ data increases with bridge width, again because the free energy barrier increases with width.

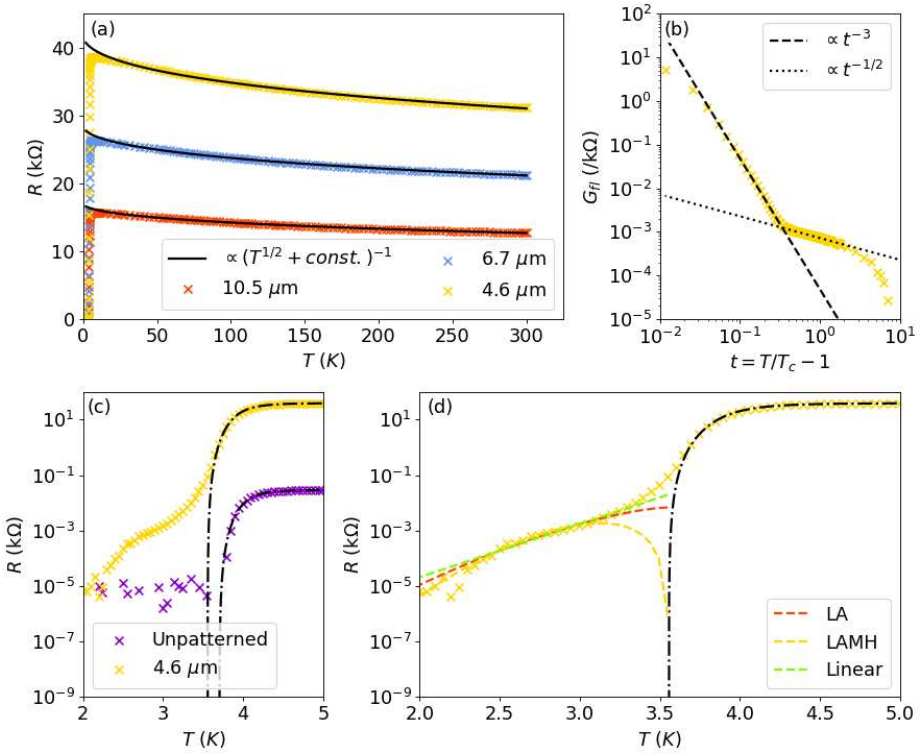

Figure 2: **Resistance as a function of temperature, $R(T)$, for BNCD microbridges - focusing on the 4.6 μm wide microbridge - and the unpatterned film. (a)** $R(T)$ for three 1600 μm long microbridges (widths as indicated by the legend) in the temperature region 2 – 300 K. The high temperature data are fit to the form $G(T) = a + b\sqrt{T}$ expected from electron-electron interaction theory. **(b)** Log-log plot of the fluctuation conductivity $G_{fl}(T)$ as a function of the reduced temperature, showing a crossover from 0D to 3D behavior at $T - T_c \sim 0.3$ K. **(c)** The superconducting transition of the unpatterned film does not show evidence of broadening below T_c. The black line is a fit to the fluctuation conductivity. The superconducting transition of the 4.6 μm wide microbridge is shown for comparison. **(d)** Low temperature $R(T)$ for the 4.6 μm wide microbridge. The resistance below T_c is fit to the LA (red), LAMH (yellow) and linear (green) forms. Note that none of these are expected to be accurate close to T_c as they assume large free energy barriers.

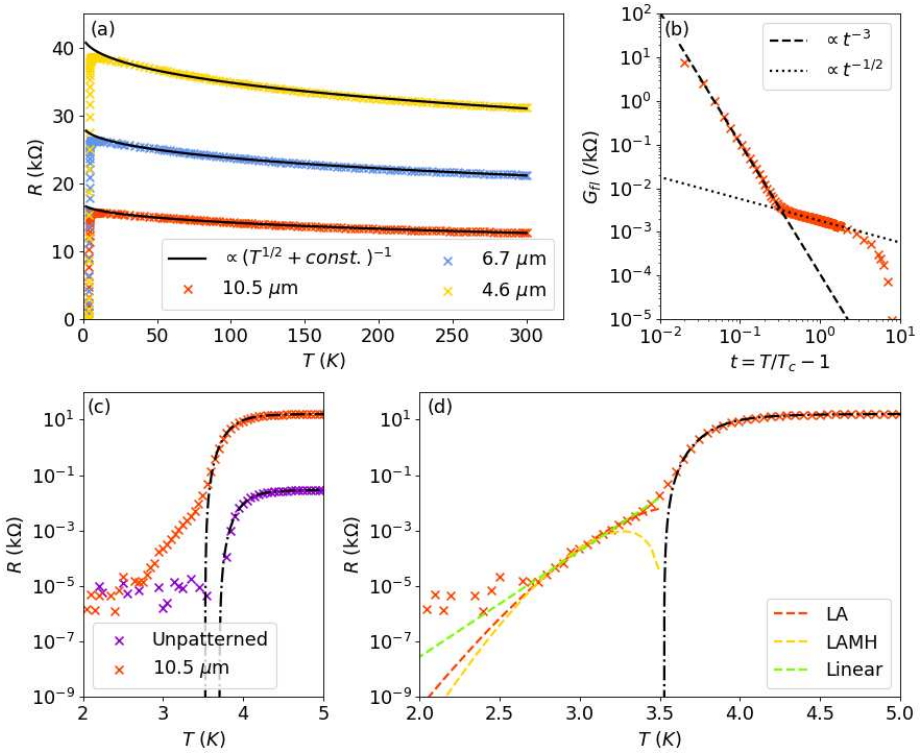

Figure 3: **Resistance as a function of temperature, $R(T)$, for BNCD microbridges - focusing on the 10.5 μm wide microbridge - and the unpatterned film. (a)** $R(T)$ for three 1600 μm long microbridges (widths as indicated by the legend) in the temperature region 2 – 300 K. The high temperature data are fit to the form $G(T) = a + b\sqrt{T}$ expected from electron-electron interaction theory. **(b)** Log-log plot of the fluctuation conductivity $G_{fl}(T)$ as a function of the reduced temperature, showing a crossover from 0D to 3D behavior at $T - T_c \sim 0.3$ K. **(c)** The superconducting transition of the unpatterned film does not show evidence of broadening below T_c. The black line is a fit to the fluctuation conductivity. The superconducting transition of the 10.5 μm wide microbridge is shown for comparison. **(d)** Low temperature $R(T)$ for the 10.5 μm wide microbridge. The resistance below T_c is fit to the LA (red), LAMH (yellow) and linear (green) forms. Note that none of these are expected to be accurate close to T_c as they assume large free energy barriers.

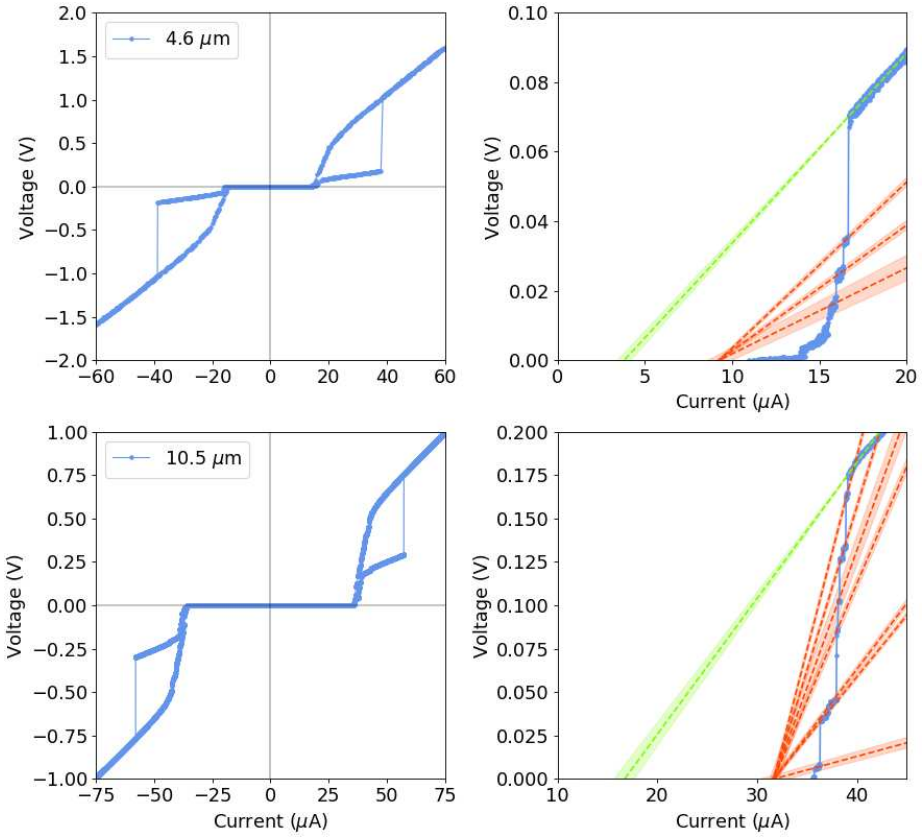

Figure 4: **Current-biased $V(I)$ characteristics for the 4.6 μm wide (top) and 10.5 μm wide (bottom) microbridges.** A detailed view of individual voltage steps for each sample, showing the converging linear slopes, is shown next to the full $V(I)$ characteristic for each sample. As with the 6.7 μm wide microbridge, there are two points of intercept on the current axis, where the lower intercept is around half of the upper.

References

[1] O. A. Williams, M. Nesladek, M. Daenen, S. Michaelson, A. Hoffman, E. Osawa, K. Haenen, R. Jackman, Growth, electronic properties and applications of nanodiamond, Diamond and Related Materials 17 (7) (2008) 1080–1088.

[2] O. A. Williams, O. Douhéret, M. Daenen, K. Haenen, E. Ōsawa, M. Takahashi, Enhanced diamond nucleation on monodispersed nanocrystalline diamond, Chemical Physics Letters 445 (4) (2007) 255–258.

[3] G. M. Klemencic, S. Mandal, J. M. Werrell, S. R. Giblin, O. A. Williams, Superconductivity in planarised nanocrystalline diamond films, Science and technology of advanced materials 18 (1) (2017) 239–244.